Journal of Materials Chemistry B

Accepted Manuscript

ROYAL SOCIETY OF CHEMISTRY

www.rsc.org/materialsB

J Mater Chem B

ARTICLE

Effects of the Molecular Weight and the Valency of Guest-modified Poly(ethylene glycol)s on the Stability, Size and Dynamics of Supramolecular Nanoparticles

Received 00th January 20xx,
Accepted 00th January 20xx

DOI: 10.1039/x0xx00000x

www.rsc.org/

Carmen Stoffelen, Eugenio Staltari-Ferraro, and Jurriaan Huskens*

The influence of the polymer length and the valency of guest-modified poly(ethylene glycol) (PEG) on the stability, size tunability and formation dynamics of supramolecular nanoparticles (SNPs) has been studied. SNPs were formed by molecular recognition between multi- and monovalent supramolecular building blocks with host or guest moieties, providing ternary complexes of cucurbit[8]uril, methyl viologen and naphthol (Np). SNP assembly was carried out using monovalent Np-modified oligo(ethylene glycol)s and PEGs with 3 or, on average, 18, 111, or 464 ethylene glycol (EG) repeat units. SNP formation and stoichiometry-controlled size tuning were observed for SNPs prepared with Np-modified PEGs containing between 18 and 464 EG repeat units, whereas no distinct assemblies were formed using the shorter Np-functionalized tri(ethylene glycol). Tentatively, the stabilization of SNPs by monovalent PEGs is partly attributed to dynamic exchange. Use of the divalent Np-functionalized PEG (with 113 EG repeat units) slowed down the SNP assembly dynamics and distinct sizes were only obtained when performing the self-assembly at 40°C for 12 h.

1. Introduction

Synthetic nanomaterials with dimensions smaller than a few hundreds of nanometers hold great promise in catalysis,[1] as analytical sensors,[2-3] and for electronic[4] or biomedical applications.[5-6] Nanoparticles (NPs) in particular can function as multifunctional diagnostic and therapeutic tools to protect and deliver active compounds to targeted tissue in vivo, while preventing their degradation and minimizing undesired side effects.[7-9]

NPs are generally not colloidally stable in biological fluids as the high surface energy of the NPs and the high ionic strength of the fluids lead to uncontrolled particle aggregation.[10] Furthermore, physiological environments such as blood, interstitial fluids or cellular cytoplasma, contain mixtures of proteins which adsorb to the NP surface by non-specific interactions.[11-12] These adsorbed proteins alter the size and interfacial composition of a nanomaterial and often act as opsonins, markers that enhance phagocytosis by the mononuclear phagocyte system (MPS).[13-14] Therefore, polymer-based steric stabilization layers are required to prevent uncontrolled protein adsorption and rapid clearance of NPs from the bloodstream to increase the pharmacokinetics and biodistribution of NPs in vivo.[15]

Surface modification with oligo(ethylene glycol) or poly(ethylene glycol) (PEG) called "pegylation" has been the most widely used method to create a steric barrier around NPs to prevent nonspecific adsorption from complex media.[16] Using this strategy, a variety of NP systems has been reported in which the in-vivo circulation time of pegylated NPs was extended compared to the uncoated parent particles.[17-18] Apparently, the PEG length[19-20] and PEG density[21] have strong, inhibiting effects on the serum protein adsorption and macrophage uptake and therefore result in increased blood circulation times.

Supramolecular nanoparticles (SNPs) are formed by multiple multivalent and monovalent building blocks brought together by specific non-covalent interactions.[22] The chemical versatility of the SNP assembly supports the inclusion of active compounds into the particles, which has been used for applications such as the delivery of RNA/DNA,[23-25] drugs,[26] imaging agents[27] or transcription factors.[28] Assembled by multivalent electrostatic or host-guest interactions in the core, the SNP formation strategy requires additional stabilization by hydrophilic polymers assembling at the SNP shell. This colloidal SNP stabilization has been achieved by host-guest interactions of cyclodextrin and adamantane using a monovalent adamantyl-functionalized PEG interacting with the multivalent CD-functionalized polymer thus constituting the SNP shell.[23-24, 26, 29-30] The shielding enabled by the PEG shell provided the stability of polycation-nucleic acid composites in biological fluids, and the long-term circulation of these SNPs in vivo.[31]

Recently, a novel SNP formation strategy was presented by us, in which the SNP assembly is promoted by multiple inclusion-assisted charge transfer complexes between cucurbit[8]uril (CB[8]), methyl viologen (MV) and naphthol (Np).[32] By

Molecular NanoFabrication Group, MESA+ Institute for Nanotechnology, University of Twente, P.O. Box 217, 7500 AE Enschede, The Netherlands
Electronic Supplementary Information (ESI) available: Detailed synthetic procedures of building blocks and analytical methods. See
DOI: 10.1039/x0xx00000x

equipping multi- and monovalent molecules with MV or Np moieties, SNPs were obtained upon assembling these building blocks in the presence of CB[8]. Because of the relatively high binding affinity of the MV-Np-CB[8] ternary complex, the assembly dynamics of the SNPs appeared to be markedly slower than that observed for cyclodextrin assemblies. Nonetheless, the interplay between multivalent and monovalent Np-bearing guest molecules provided size tuning of the SNPs similar to the SNP formation strategy reported by Tseng and coworkers for the interaction of cyclodextrin and adamantyl-functionalized building blocks.[30] In the CB[8] and CD strategies, both the colloidal stability as well as the size tuning of the SNPs is attributed to the shielding effect of the monovalent guest-modified PEG stopper. But it is unclear to which extent the polymer length and the valency of the stopper affect the SNP shielding.

The aim of the work presented here is to correlate the structure of the guest-modified PEG stopper with the colloidal stability, size tuning and assembly dynamics of SNPs stabilized by CB[8]/MV/Np interactions. In particular, the effects of the length of the PEG chain and the number (valency) of guest moieties attached to the PEG end on the SNP stability are evaluated in detail.

2. Materials and Methods

2.1 Reagents

Chemicals were obtained from commercial sources and used as such. Octa-(*E*)-5-naphthol-pentanoic-acid poly(amido amine) dendrimer (generation 1) (Np_8-PAMAM), methyl viologen-functionalized poly(ethylene imine) (MV-PEI) and naphthalene poly(ethylene glycol) methyl ether (Np-PEG_{111}) were synthesized as described.[32] Cucurbit[8]uril (CB[8]) was purchased and its purity was assessed by microcalorimetric titration against paraquat. Millipore water with a resistivity of 18.2 MΩcm^{-1} was used for dialysis and SNP preparation.

2.2 SNP formation using different shell components

As schematically shown in Scheme 1, SNPs are formed by the self-assembly of MV-poly(ethylene imine) (MV-PEI), Np-poly(amido amine) dendrimer (Np_8-PAMAM), CB[8] and different Np-functionalized PEGs. In the presence of CB[8], the SNPs assemble by multiple interactions of MV-PEI and Np_8-PAMAM in the particle core and of Np-PEG in the SNP shell. In our previous study[32] we showed, in particular for Np-PEG_{111}, that the SNP formation is based on the instantaneous and complete formation of CB[8]-assisted, ternary, charge-transfer complexes between the CB[8], MV and Np units, that were attached to the multivalent and monovalent building blocks, and were employed in a 1:1:1 stoichiometry. Using monovalent Np-conjugated PEG with different lengths, the effect of the polymer length on the formation of SNPs is evaluated in the current study. Furthermore, the effect of the valency of the PEG stopper is tested by using a divalent Np-conjugated PEG with a polymer length comparable to that of the monovalent derivative described for the formation of

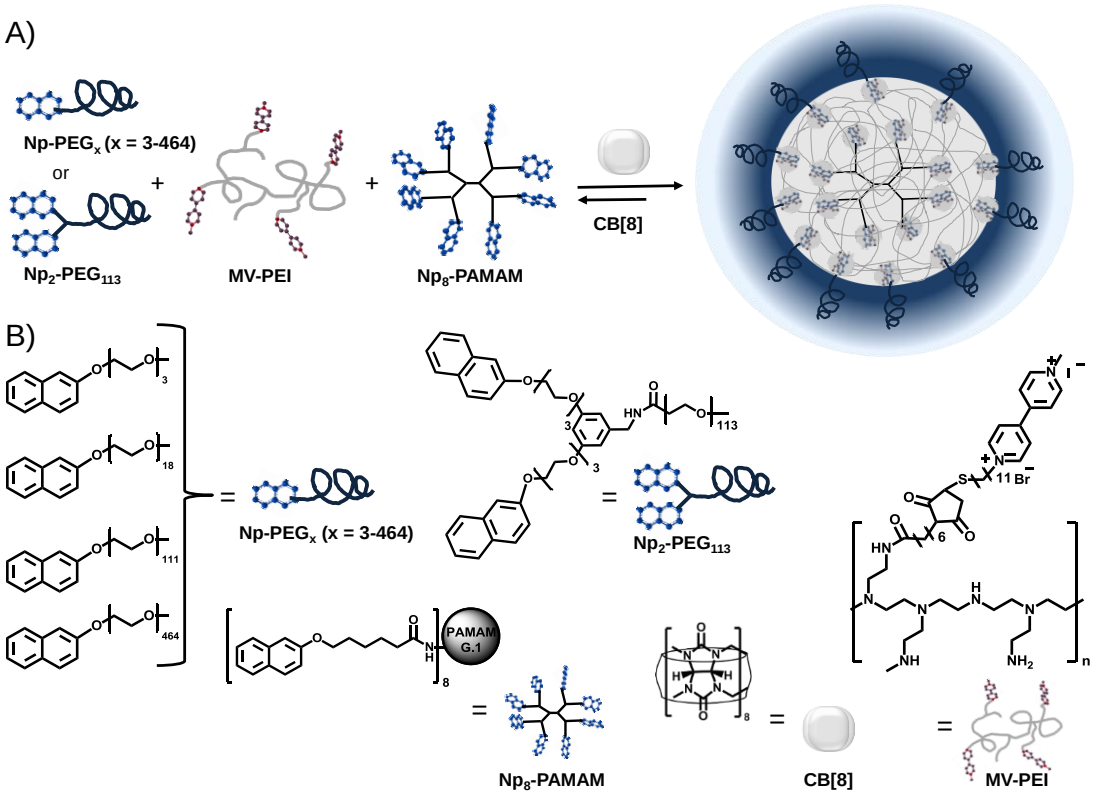

Scheme 1 A) Supramolecular nanoparticle (SNP) formation by heteroternary complex formation between cucurbit(8)uril (CB[8]), methyl viologen (MV) and naphthol (Np) moieties using MV-poly(ethylene imine) (MV-PEI), Np-functionalized PAMAM G1 dendrimer (Np_8-PAMAM), CB[8] and different Np-functionalized poly(ethylene glycol)s (Np-PEGs). B) The supramolecular building blocks used for SNP formation: Np-tri(ethylene glycol) (Np-PEG_3), Np-PEG_{18}, Np-PEG_{111}, Np-PEG_{464}, Np_2-PEG_{113}, MV-PEI, Np_8-PAMAM and CB[8].

previously reported supramolecular nanoparticles.[32]

2.3 Synthesis of the different naphthol-terminated PEG derivatives

To study the effect of PEG length on SNP formation, various Np-conjugated PEG stopper molecules were synthesized. Next to four monovalent Np-conjugated PEG derivatives, with 3 or, on average, 18, 111, or 464 repeat units, also a divalent Np-grafted PEG, Np_2-PEG_{113}, was synthesized. As shown in Scheme 2, the short Np-PEG_3 was synthesized by the reaction of 2-naphthol with NaH followed by Williamson ether synthesis using chloro-ethoxy-ethoxy-ethanol. Np-PEG_{18} was synthesized as Np-PEG_{111} by a substitution reaction of 2-naphthol with poly(ethylene glycol) methyl ether tosylate. The longest monovalent Np-conjugated PEG, Np-PEG_{464} was prepared by reaction of 2-naphthoylchloride with PEG methyl ether amine in dichloromethane. To prepare Np_2-PEG_{113} (Scheme 2D), first the hydroxyl group of Np-PEG_3 was converted to the more reactive bromide using PBr_3 in toluene. This bromide (**4**) was reacted with 3,5-dihydroxy benzonitrile under reflux using K_2CO_3 and 18-crown-6 in acetone to obtain the divalent guest unit 5. The nitrile functionality of **5** was converted to an amine by the hydrogenation with H_2 in the presence of Raney-nickel as the catalyst. In the final step, Np_2-PEG_{113} (**6**) was obtained by reaction with methyl-poly(ethylene glycol) *N*-hydroxysuccinimide ester in CH_2Cl_2.

2.4 SNP formation with different Np-conjugated PEG derivatives

The formation of SNPs was studied using a 0.67 µM concentration of CB[8], MV and Np, while keeping the molecular recognition moieties in a stoichiometric ratio of 1:1:1. Therefore, Np_8-PAMAM was dissolved in DMSO and aqueous solutions of MV-PEI, CB[8] and Np-PEG_x (x = 3, 18, 111, 464) or the divalent Np_2-PEG_{113} were prepared prior to mixing. Size tuning of the SNPs was assessed by varying the concentrations of the Np conjugated PEG derivative and the Np_8-PAMAM dendrimer, while keeping the overall concentration of the Np moieties constant. The Np_x-conjugated PEG_x was mixed with Np_8-PAMAM and CB[8] prior to addition of MV-PEI. Although it is known that the hetero-ternary complex formation between MV, Np and CB[8] occurs instantaneously upon mixing of the building blocks[32,33] we have shown that stable SNPs are formed more slowly by the necessary exchange of the MV and Np moieties via dissociation and reassociation, taking up to a few days to form well-defined nanoparticles.[32] To ensure stable SNP formation in the current study, all prepared SNP formulations were evaluated by DLS and SEM 2 or 7 days after mixing, respectively, which has been shown to be sufficient for stable particle formation.

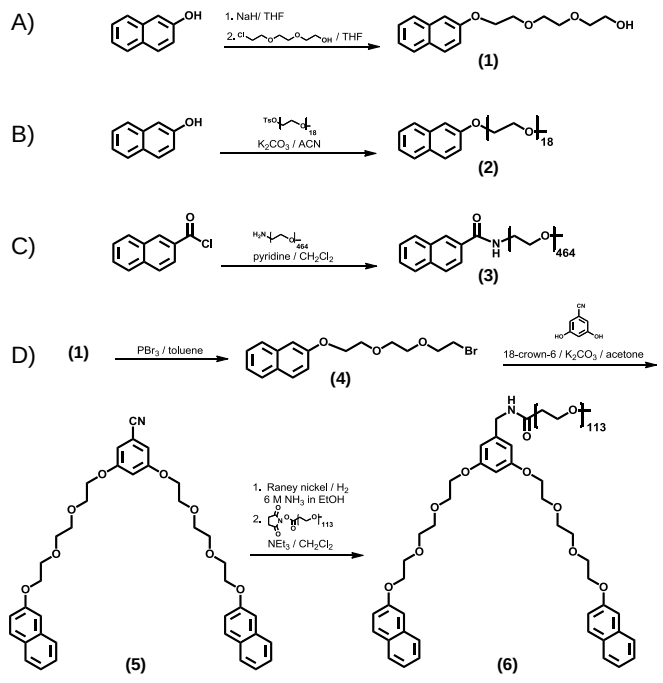

Scheme 2 Synthesis routes towards the (A-C) monovalent Np-conjugated PEG derivatives and (D) the divalent Np_2-PEG_{113} used in this study.

3. Results and Discussion

3.1 SNP formation with monovalent Np-PEG of varying length

As is visible in Fig. 1A-C, self-assembly experiments carried out with Np-PEG_3, Np_8-PAMAM, MV-PEI and CB[8] did not result in

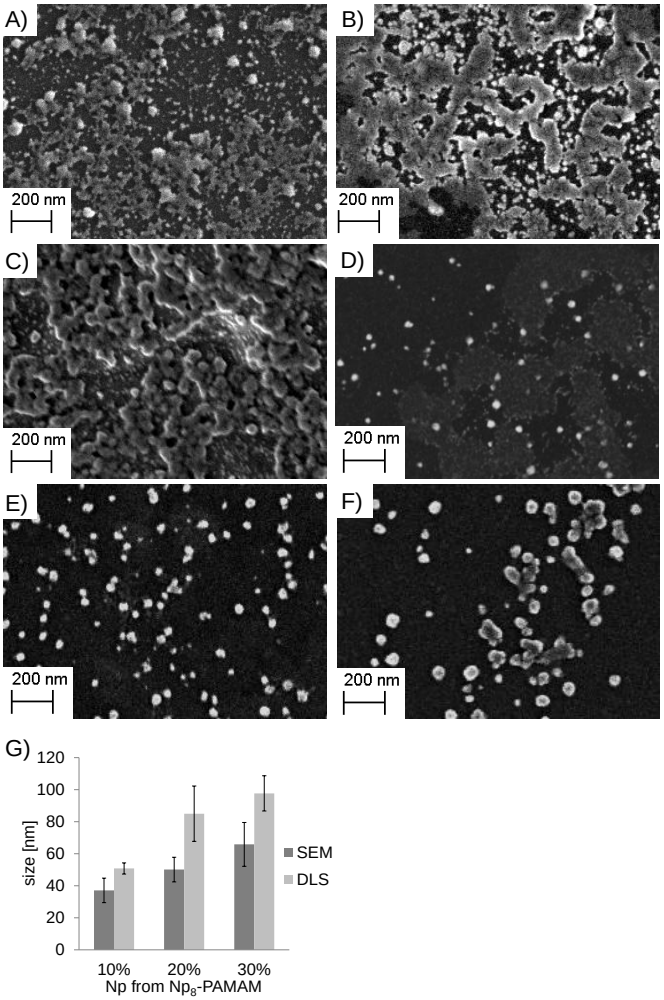

Fig. 1 Size determinations of SNPs prepared with Np-PEG_3 (A-C) and Np-PEG_{18} (D-G). SEM images (A-F) as a function of the Np content derived from Np_8-PAMAM dendrimer (A: Np-PEG_3 10%, B: Np-PEG_3 20%, C: Np-PEG_3 30%, D: Np-PEG_{18} 10%, B: Np-PEG_{18} 20%, C: Np-PEG_{18} 30%) used during supramolecular assembly while keeping the concentration of CB[8]:MV:Np = 1:1:1. G) SNP diameter of SNPs prepared with Np-PEG_{18} as measured by SEM and DLS.

distinct SNP formation. Only few particle-shaped structures were visible embedded in large amounts of aggregated organic material. This observation is underlined by the DLS analysis carried out for this SNP formulation. Regardless the concentration of Np_8-PAMAM used during the self-assembly experiments, only irreproducible measurements and no distinct particle formation was observed by DLS, which is attributed to severe aggregation.

In contrast, distinct SNPs were observed by SEM and DLS (Fig. 1D-G) for self-assembly experiments carried out with Np-PEG_{18}, Np_8-PAMAM, MV-PEI and CB[8]. By increasing the amount of Np derived from Np_8-PAMAM, while decreasing the amount Np from Np-PEG_{18}, the observed SNP size increased from 37 ± 7 nm to 65 ± 13 nm as measured by SEM and from 50 ± 3 nm to 97 ± 11 nm as analyzed by DLS.

As seen in Fig. 2, distinct SNPs were formed as well for different formulations using Np-PEG_{464}, Np_8-PAMAM, MV-PEI and CB[8]. Also in this case, stoichiometric size control was observed by increasing the amount of Np from Np_8-PAMAM from 10% to 30%, while decreasing the amount of Np-PEG_{464} from 90% to 70% correspondingly: an increase in SNP size was observed from 35 ± 4 nm to 61 ± 12 nm by SEM and from 47 ± 9 nm to 117 ± 15 nm by DLS (Fig. 2D).

Summarizing, the results shown above illustrate that distinct SNP formation is not possible using Np-PEG_3 as the stopper assembling in the shell of the SNPs. Most likely the short tri(ethylene glycol) moiety does not provide sufficient stability to the SNPs, because of its marginal steric shielding capacity. Including the results previously reported[32] for Np-PEG_{111}, clear SNP formation was observed for SNPs formed using Np-PEG_{18}, Np-PEG_{111} and Np-PEG_{464}. Remarkably, even the still fairly short Np-PEG derivative grafted with 18 repeat units is apparently capable of providing sufficient colloidal stability to the SNPs. Furthermore, for all SNPs, size tuning was obtained by stoichiometric control of the ratio between the multivalent and monovalent Np components, irrespective of the length of the Np-PEG.

Fig. 3 shows a comparison of the particle sizes determined by DLS (Fig. 3A) and SEM (Fig. 3B). Whereas the SEM diameters show no dependence on PEG length, the hydrodynamic diameters measured by DLS show a slightly upward trend for increasing chain lengths. Also the differences between DLS and SEM sizes (Fig. 3C) increase with an increase of the fraction of multivalent Np dendrimer. In all cases, the effect of PEG length on particle size seems to be statistically insignificant.

It has been reported that the surface area occupied by PEG increases with the length of the polymer.[34] When assuming that a PEG stopper is attached to the SNP surface in a mushroom conformation and that the particles are dispersed in aqueous solution, the average diameter of the PEG coil ($\xi_{mushroom}$) assembled onto the SNP surface can be calculated by $\xi_{mushroom} = 0.76\times(M_{w(PEG)})^{0.5}$ with $M_{w(PEG)}$ the molecular weight of the PEG chain and the area of SNP covered by the polymer with $A_{mushroom} = \pi\times(\xi_{mushroom}/2)^2$.[34] Taking into account that the SNPs are surrounded by PEG, we estimate that the average SNP diameter in water, compared to SNPs made using Np-PEG_{18}, would increase by 6 nm for SNPs assembled with

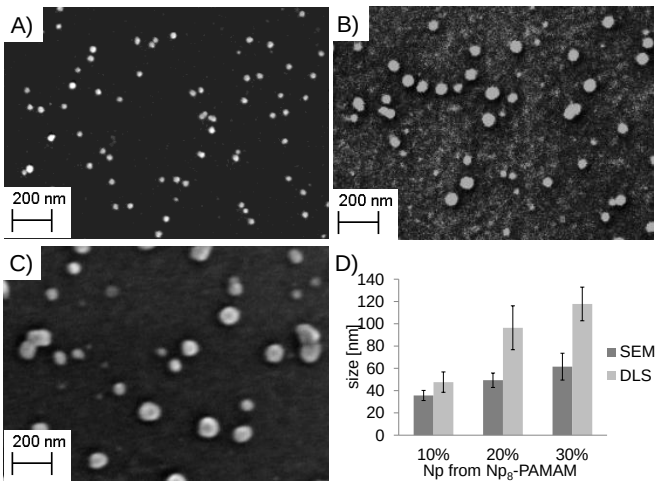

Fig. 2 Size determinations of SNPs prepared with Np-PEG_{464}: SEM images (A-C) as a function of the Np content derived from Np_8-PAMAM dendrimer (A: 10%, B: 20%, C: 30%) used during supramolecular assembly while keeping the concentration of CB[8]:MV:Np = 1:1:1. D) SNP diameter as measured by SEM and DLS.

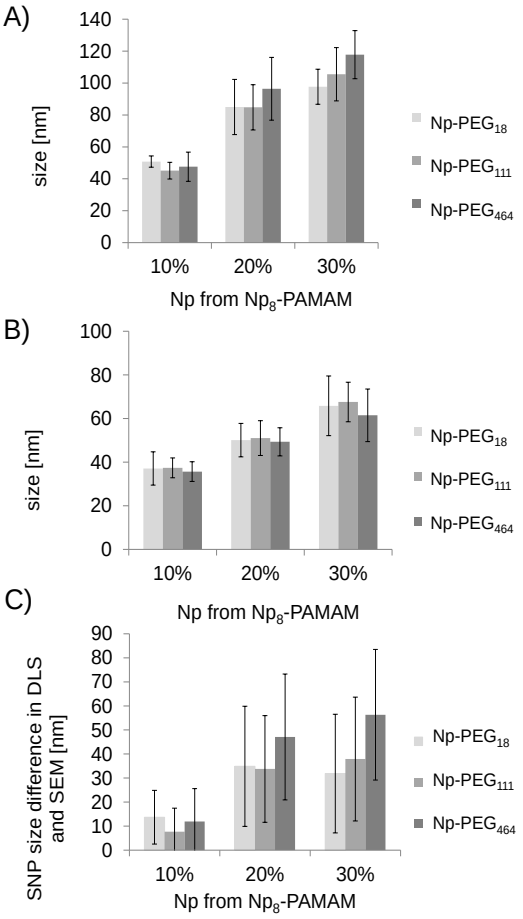

Fig. 3 Size determinations of SNPs prepared with Np-PEG_{18} (■), Np-PEG_{111} (■) and Np-PEG_{464} (■): A) by DLS and B) by SEM. C) Difference in hydrodynamic diameter by DLS and SNP diameter by SEM.

Np-PEG_{111} or even with 17 nm for SNPs assembled with Np-PEG_{464}. The data shown in Fig. 3 do not contradict with these calculations, but the size distributions are too broad to give a firm experimental confirmation.

By formation of SNPs with PEGs of larger chain lengths, the PEG chains require a larger surface area per chain, so less PEG chains are required to occupy the SNP surface and to stabilize the assembly. From this, it can be expected that an increasing fraction of stopper remains unused, and creates a thermodynamic driving force for the formation of smaller (by core) SNPs. As support for this, it can be estimated from the binding constant of Np with the preformed CB[8]/MV complex ($(6.1\pm0.5)\times10^5$ M^{-1})[35] and the low building block concentration used for SNP formation (0.7 µM), that maximally only ~42% of the Np-PEG molecules are assembled onto the SNP surface and the residual PEG chains are free in solution. This percentage is decreasing upon increase of the length of the PEG chain, indicating a lower number of PEG stopper molecules attached onto the SNP surface. This could explain the increasing difference between DLS and SEM sizes indicated in Fig. 3C. The SNPs prepared with the longest PEG chains show the largest loss of water upon drying, which is related to a higher hydration of the SNPs, a larger content of PEG and possibly a lower content of stopper.

Overall, as we cannot observe a clear size increase or decrease by the formation of SNPs with different PEG lengths, we assume that both mechanisms could be playing a combined and counteracting role in the determination of the SNP size by self-assembly. Although the mushroom conformation of the longer PEG chains attached onto the SNP surface is larger, the SNP core shrinkage due to the occupation of more space by PEG could lead to a negligible size difference between the SNPs prepared with different PEG lengths.

By taking an even closer look to the composition and configuration of the SNPs, the often proclaimed effect of steric stabilization by monovalent Np-PEGs becomes obscure. Assuming that the SNPs are formed by 90% water and 10% organic material and knowing that that a single CB[8] has an projected surface area of 3 nm^2,[36] one CB[8] molecule is assembled for each approx. 30 nm^2 of SNP surface area. Furthermore, including that only 42% of the Np-PEG interacts with the CB[8]/MV complexes gives that a single Np-PEG polymer chain is assembled onto each 71 nm^2 of SNP surface. By taking the mushroom conformational area into account occupied by the different Np-PEGs (Table 1), it is obvious that only the SNPs prepared with Np-PEG_{464} contain a shell in which the polymer chains feel each other and in which a dense PEG coverage is ensured. Therefore only for these SNPs a lower number of PEG molecules might be assembled onto the SNP surface, whereas all other SNPs are formed by the same amount of Np-PEG chains, verifying the results shown in Fig. 3. On the other extreme, Np-PEG_{18} provides colloidal stability even though only about 5% of the SNP surface area is covered by PEG in this case.

Thus, it can be assumed that the Np-PEGs with shorter PEG length provide only marginal polymer shielding of the SNPs. Therefore, we propose that the SNPs are additionally stabilized by a dynamic effect in which the Np-PEGs are hopping between the different CB[8] host positions available on the SNP surface and thereby provide additional colloidal stabilization. As studied before, the exchange rate of individual, monovalent Np units at the Np-MV-CB[8] complex is determined by a dissociation rate constant on the order of 10 s^{-1}.[37] This indicates that a single Np-PEG chain could dissociate and rebind to a free MV-CB[8] site several times per second.

Table 1 Polymer diameter and area of PEG with different PEG length assembled in mushroom conformation onto the particles surfaces.

PEG deriv.	$M_{w(PEG)}$ (g/mol)	$\xi_{mushroom}$ (nm)	$A_{mushroom}$ (nm^2)
Np-PEG_3	133	0.9	0.6
Np-PEG_{18}	801	2.2	3.6
Np-PEG_{111}	4884	5.3	22.2
Np-PEG_{464}	20416	10.9	92.6

3.2 Supramolecular nanoparticle formation with stoppers of different valencies

To study the effect of the valency of the stopper on the SNP formation, also the divalent Np_2-PEG_{113} was synthesized and used for SNP formation. In accordance with the previous experiments, Np_2-PEG_{113}, Np_8-PAMAM, MV-PEI and CB[8] were mixed, and SNP formation was evaluated by SEM and DLS after keeping the samples for 2 and 7 days, respectively, at room temperature. As two Np groups are grafted onto the divalent Np_2-PEG_{113}, only half of the molar concentration of the stopper, in comparison to the monovalent Np-PEGs, was used for SNP formation to keep the concentrations of host and guest moieties equimolar.

As visible in the SEM images shown in Fig. 4, self-assembly of

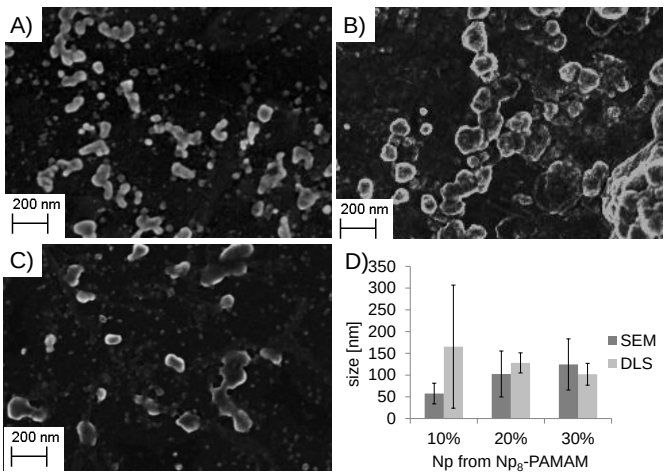

Fig. 4 Size determinations of SNPs prepared with Np_2-PEG_{113} at RT: SEM images 7 days after self-assembly (A-C) as a function of the Np content derived from Np_8-PAMAM dendrimer (A: 10%, B: 20%, C: 30%) used during supramolecular assembly while keeping the concentration of CB[8]:MV:Np = 1:1:1. D) SNP diameter as measured by SEM and DLS.

the supramolecular building blocks led to the formation of supramolecular particle-like assemblies for different dendrimer-stopper ratios, but the shape of these SNPs was not as spherical as observed for SNPs prepared with Np-PEG_{113}.[32] This is witnessed by the absence of stable and reproducible DLS readings for the SNPs prepared with 10% Np from Np_8-PAMAM and the occurrence of heterogeneous structures by SEM for the samples prepared with 20% and 30% Np from Np_8-PAMAM.

To evaluate whether the SNP heterogeneity is a result of slow dynamics, time-dependent DLS measurements were carried out at RT and at 40°C. As seen in Fig. 5, the observed hydrodynamic diameter of the SNPs containing 25% Np from Np_8-PAMAM varied with temperature and with the valency of the Np-functionalized PEG. As shown before,[32] the size of the SNPs prepared with Np-PEG_{111} is stabilized at 40°C within 4 to 6 h. Prolonged (over 28 h) heating, however, led to SNP aggregation. This behavior is tentatively attributed to accelerated multivalent binding of the SNP core components at elevated temperature, whereas the fast association and dissociation of the monovalent Np-PEG_{111} apparently does not provide sufficient SNP stabilization over time. In contrast, SNPs formed with Np_2-PEG_{113} showed a reproducible size with low standard deviations after 12 to 14 h at 40°C, and were stable during the whole monitoring time (40 h). This is expected as dissociation of the bivalent Np_2-PEG_{113} is markedly slower than the dissociation of the monovalent Np-PEG_{111} which leads to higher stability of the SNPs at elevated temperatures. At RT, however, the samples prepared with Np_2-PEG_{113} were not as consistent as the samples prepared at 40°C and the standard deviations remained relatively high, even 35 h after mixing.

Subsequently, the size tunability of the SNPs formed with Np_2-PEG_{113} was evaluated by preparing the SNP samples at 40°C instead of at RT. Hereto, the supramolecular building blocks were mixed and kept at 40°C for 10 h followed by 1 d at RT prior to characterization. As visible in Fig. 6, more distinct and spherical SNPs were observed by SEM. Furthermore, SEM and DLS size determinations show clearly the characteristic stoichiometric size control by varying the content of divalent and multivalent Np-bearing building blocks. In particular, by increasing the amount of Np from Np_8-PAMAM from 10% to 30%, while decreasing the amount of Np from Np_2-PEG_{113} from 90% to 70% correspondingly, an increase in SNP size was observed from 60 ± 10 nm to 86 ± 16 nm by SEM and from 88 ± 9 nm to 144 ± 36 nm by DLS (Fig. 6D).

Taken together, the time and temperature-dependent DLS measurements and the stoichiometry controlled SNP assembly show that an elevated temperature is required to form SNPs with distinct sizes and homogeneous shapes for SNPs prepared with the divalent Np_2-PEG_{113} as the stopper. As described in earlier,[32] SNP self-assembly requires the dynamic disassembly and reassembly of the four supramolecular building blocks for well-defined SNP formation. By using a divalent instead of monovalent guest-modified PEG, this dynamic process is slowed down. This is in agreement with the observations and predictions that the overall dissociation rate of a guest molecule decreases by increasing its valency.[38-41]

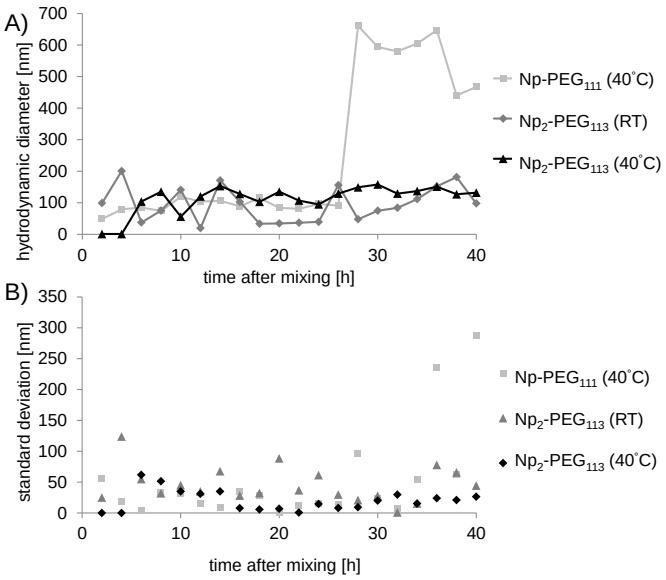

Fig. 5 A) Hydrodynamic diameters of SNPs prepared with Np-PEG_{111} or Np_2-PEG_{113}, consisting of 25% Np from Np_8-PAMAM measured by time-dependent DLS as a function of temperature averaged over four measurements and B) corresponding standard deviations.

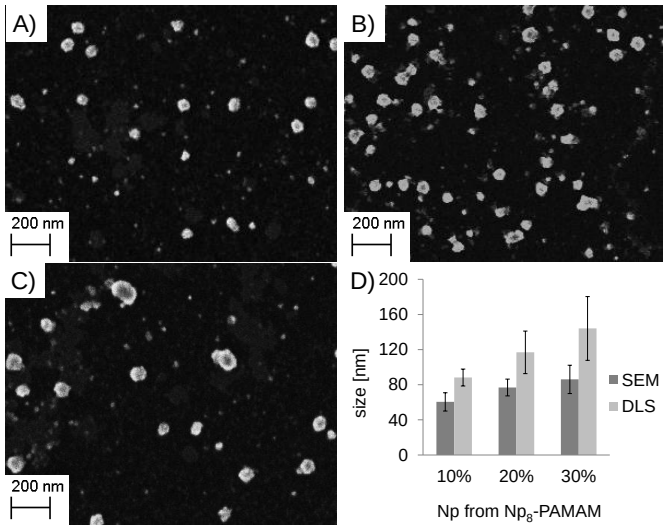

Fig. 6 Size determinations of SNPs prepared with Np_2-PEG_{113} at 40°C: SEM images (A-C) as a function of the Np content derived from Np_8-PAMAM dendrimer (a: 10%, b: 20%, c: 30%) used during supramolecular assembly while keeping the concentration of CB[8]:MV:Np = 1:1:1. D) SNP diameter as measured by SEM and DLS.

For SNPs formed using the divalent stopper, the effective molarity (EM) - which is the probability of the second Np moiety of an already monovalently interacting divalent guest to find another available host molecule at the SNP surface - determines the thermodynamic and kinetic multivalent stopper effects. We estimate the effective molarity on an SNP surface to be about 1 mM, which is similar to the EM of a divalent adamantyl derivative binding to a cyclodextrin (CD) dimer.[39] Although the size of CB[8] is comparable to CD, taking the value for a densely CD-coated surface (100 mM)[39] is likely

to be too high for SNPs, as the SNP surface is not expected to be close packed (10% seems more realistic) and not all MV moieties are complexed with CB[8].[40] This, together with the binding constant of ((6.1±0.5)×10^5 M^{-1})[35] for a Np unit binding to MV-CB[8], leads to the estimation that the dissociation rate constant of the divalently bound stopper is 2-3 orders of magnitude lower than that of a monovalent one. This explains the observed slower formation at RT, although an exact timeframe for stable particle formation can currently not be set.

The time-dependent measurements at 40°C indicate the slowing down of the dynamics upon increasing the stopper valency from one to two with less than an order of magnitude at this temperature. It seems unlikely that such a small difference in temperature could cause a large change in binding affinity and effective molarity. Therefore, the limited decrease of the observed equilibration time probably indicates that the equilibration process is to a large extent dictated by the valency of the core dendrimer rather than the stopper, although the valency of the stopper has an unmistaken effect on the dynamics.

Notably, the SNPs formed by 10% to 30% Np from Np_8-PAMAM and stabilized by the divalent Np_2-PEG_{113} stopper are larger (88 ± 9 nm to 144 ± 36 nm) than the SNPs assembled with the monovalent Np-PEG_{111} (51 ± 13 nm to 107 ± 16 nm). Yet, the surface coverage of the PEGs with the different valency does not explain the difference in observed SNP size. Even by assuming that Np_2-PEG_{113} completely binds to all CB[8] hosts assembled in the SNP shell, the SNP surface area is not completely covered by PEG and the individual polymer chains do not interact with each other, which is comparable to the SNPs prepared with Np-PEG_{111}. More likely, the divalent character of Np_2-PEG_{113} causes the divalent guest to take part, to some extent, in the crosslinking of the supramolecular building blocks in the core, similar to the previously observed aggregation of CD-functionalized gold NPs with a bis-adamantyl guest molecule in solution.[42] In this way, use of the divalent stopper may lead to an increased SNP size.

4. Conclusions

SNPs stabilized by inclusion-assisted ternary charge transfer complexes between CB[8], MV and Np can be assembled using different Np-modified PEGs. No difference in formation and size tunability was observed for SNPs prepared with Np-PEG_{18}, Np-PEG_{111} or Np-PEG_{464}, whereas no clear SNP formation was observed for SNPs prepared with the short Np-functionalized tri(ethylene glycol). From a comparison of the PEG size and the expected coverage of the SNP surface with ternary complexes, a dense packing of the PEG chains is only expected for the highest PEG length. We tentatively attribute the stabilization of SNPs with short PEGs to dynamic assembly and reassembly of the monovalent Np-functionalized PEGs, whereas steric effects provide some additional steric bulk, combined leading to colloidal stability of the SNPs. In contrast to the monovalent Np-PEGs, the use of the divalent Np_2-PEG requires an increased temperature to form size-tunable SNPs with distinct sizes. The apparent slowing down of the formation kinetics is due to the slower dissociation rate constant of the stopper, but the overall formation dynamics is to a large extent controlled by the multivalent core components.

In a larger context, a better understanding of the colloidal stability and assembly dynamics of supramolecular nanoparticles stabilized by guest-functionalized PEGs will be beneficial for the development of functional delivery vectors that can be used in therapeutics. Controlling the dynamics of the stopper molecules of SNPs, which is a function of interaction motif, binding affinity, exchange dynamics, PEG size and valency, is paramount to controlling the release of cargo embedded in these particles.

Acknowledgements

This work was supported by the Netherlands Organization for Scientific Research (NWO-CW; Vici grant 700.58.443 to J.H)

Notes and references

1 Z.-Y. Zhou, N. Tian, J.-T. Li, I. Broadwell, S.-G. Sun, *Chem. Soc. Rev.* 2011, **40**, 4167-4185.
2 S. Guo, E. Wang, *Nano Today* 2011, *6*, 240-264.
3 H. Jiang, *Small* 2011, **7**, 2413-2427.
4 D. Jariwala, V. K. Sangwan, L. J. Lauhon, T. J. Marks, M. C. Hersam, *Chem. Soc. Rev.* 2013, **42**, 2824-2860.
5 Y. Xia, *Nat. Mater.* 2008, **7**, 758-760.
6 J. L. West, N. J. Halas, *Annu. Rev. Biomed. Eng.* 2003, **5**, 285-292.
7 L. Zhang, F. X. Gu, J. M. Chan, A. Z. Wang, R. S. Langer, O. C. Farokhzad, *Clin. Pharmacol. Ther.* 2007, **83**, 761-769.
8 C. Sun, J. S. H. Lee, M. Zhang, *Adv. Drug Delivery Rev.* 2008, **60**, 1252-1265.
9 I. Brigger, C. Dubernet, P. Couvreur, *Adv. Drug Delivery Rev.* 2002, **54**, 631-651.
10 Y. Min, M. Akbulut, K. Kristiansen, Y. Golan, J. Israelachvili, *Nat. Mater.* 2008, **7**, 527-538.
11 D. Walczyk, F. B. Bombelli, M. P. Monopoli, I. Lynch, K. A. Dawson, *J. Am. Chem. Soc.* 2010, **132**, 5761-5768.
12 T. Cedervall, I. Lynch, S. Lindman, T. Berggård, E. Thulin, H. Nilsson, K. A. Dawson, S. Linse, *Proc. Natl. Acad. Sci. USA* 2007, **104**, 2050-2055.
13 M. Mahmoudi, I. Lynch, M. R. Ejtehadi, M. P. Monopoli, F. B. Bombelli, S. Laurent, *Chem. Rev.* 2011, **111**, 5610-5637.
14 C. D. Walkey, W. C. W. Chan, *Chem. Soc. Rev.* 2012, **41**, 2780-2799.
15 S.-D. Li, L. Huang, *Mol. Pharmaceutics* 2008, **5**, 496-504.
16 R. A. Petros, J. M. DeSimone, *Nat. Rev. Drug Discovery* 2010, **9**, 615-627.
17 R. Gref, Y. Minamitake, M. T. Peracchia, V. Trubetskoy, V. Torchilin, R. Langer, *Science* 1994, **263**, 1600-1603.
18 J. V. Jokerst, T. Lobovkina, R. N. Zare, S. S. Gambhir, *Nanomedicine* 2011, **6**, 715-728.
19 B. Ballou, B. C. Lagerholm, L. A. Ernst, M. P. Bruchez, A. S. Waggoner, *Bioconjugate Chem.* 2003, **15**, 79-86.

20 S. D. Perrault, C. Walkey, T. Jennings, H. C. Fischer, W. C. W. Chan, *Nano Lett.* 2009, **9**, 1909-1915.
21 C. D. Walkey, J. B. Olsen, H. Guo, A. Emili, W. C. W. Chan, *J. Am. Chem. Soc.* 2011, **134**, 2139-2147.
22 K.-J. Chen, M. A. Garcia, H. Wang, H.-R. Tseng, in *Supramolecular Chemistry*, John Wiley & Sons, Ltd, 2012.
23 Y. Ping, C. Liu, Z. Zhang, K. L. Liu, J. Chen, J. Li, *Biomaterials* 2011, **32**, 8328-8341.
24 M. E. Davis, J. E. Zuckerman, C. H. J. Choi, D. Seligson, A. Tolcher, C. A. Alabi, Y. Yen, J. D. Heidel, A. Ribas, *Nature* 2010, **464**, 1067-1070.
25 H. Wang, K.-J. Chen, S. Wang, M. Ohashi, K.-i. Kamei, J. Sun, J. H. Ha, K. Liu, H.-R. Tseng, *Chem. Commun.*2010, **46**, 1851-1853.
26 K.-J. Chen, L. Tang, M. A. Garcia, H. Wang, H. Lu, W.-Y. Lin, S. Hou, Q. Yin, C. K. F. Shen, J. Cheng, H.-R. Tseng, *Biomaterials* 2012, **33**, 1162-1169.
27 K.-J. Chen, S. M. Wolahan, H. Wang, C.-H. Hsu, H.-W. Chang, A. Durazo, L.-P. Hwang, M. A. Garcia, Z. K. Jiang, L. Wu, Y.-Y. Lin, H.-R. Tseng, *Biomaterials* 2011, **32**, 2160-2165.
28 Y. Liu, H. Wang, K.-i. Kamei, M. Yan, K.-J. Chen, Q. Yuan, L. Shi, Y. Lu, H.-R. Tseng, *Angew. Chem. Int. Ed.* 2011, **50**, 3058-3062.
29 S. Mishra, P. Webster, M. E. Davis, *Eur. J. Cell Biol.* 2004, **83**, 97-111.
30 H. Wang, S. Wang, H. Su, K.-J. Chen, A. L. Armijo, W.-Y. Lin, Y. Wang, J. Sun, K.-i. Kamei, J. Czernin, C. G. Radu, H.-R. Tseng, *Angew. Chem. Int. Ed.* 2009, ***48***, 4344-4348.
31 M. E. Davis, *Mol. Pharmaceutics* 2009, *6*, 659-668.
32 C. Stoffelen, J. Huskens, *Chem. Commun.* 2013, **49**, 6740-6742.
33 H.-J. Kim, J. Heo, W. S. Jeon, E. Lee, J. Kim, S. Sakamoto, K. Yamaguchi, K. Kim, *Angew. Chem. Int. Ed.* 2001, **40**, 1526-1529.
34 S. J. Budijono, B. Russ, W. Saad, D. H. Adamson, R. K. Prud'homme, *Coll. Surf. A* 2010, **360**, 105-110.
35 U. Rauwald, F. Biedermann, S. p. Deroo, C. V. Robinson, O. A. Scherman, *J. Phys. Chem. B* 2010, **114**, 8606-8615.
36 J. Lagona, P. Mukhopadhyay, S. Chakrabarti, L. Isaacs, *Angew. Chem. Int. Ed.* 2005, **44**, 4844-4870.
37 A. Gomez-Casado, A. Gonzalez-Campo, Y. Zhang, X. Zhang, P. Jonkheijm, J. Huskens, *Polymers* 2013, **5**, 269-283.
38 J. Huskens, A. Mulder, T. Auletta, C. A. Nijhuis, M. J. W. Ludden, D. N. Reinhoudt, *J. Am. Chem. Soc.* 2004, **126**, 6784-6797.
39 A. Gomez-Casado, H. H. Dam, M. D. Yilmaz, D. Florea, P. Jonkheijm, J. Huskens, *J. Am. Chem. Soc.* 2011, **133**, 10849-10857.
40 A. Perl, A. Gomez-Casado, D. Thompson, H. H. Dam, P. Jonkheijm, D. N. Reinhoudt, J. Huskens, *Nat. Chem.* 2011, **3**, 317-322.
41 A. Mulder, T. Auletta, A. Sartori, S. Del Ciotto, A. Casnati, R. Ungaro, J. Huskens, D. N. Reinhoudt, *J. Am. Chem. Soc.* 2004, **126**, 6627-6636.
42 O. Crespo-Biel, A. Jukovic, M. Karlsson, D. N. Reinhoudt, J. Huskens, *Isr. J. Chem.* 2005, **45**, 353-362.

TOC

The length and valency of PEG-based stopper molecules have a pronounced effect on the self-assembly, size, stability and dynamics of supramolecular nanoparticles.